Supplementary Information

Hydrophobic paraffins-selective pillared-layer MOFs for olefin purification

Sisi Jiang[a,‡], Jiaqi Li[a,‡], Meng Feng[a], Rundao Chen[a], Lidong Guo[a],

Qianqian Xu[a], Lihang Chen[a,b], Fuxing Shen[a,b], Zhiguo Zhang[a,b], Yiwen Yang[a,b],

Qilong Ren[a,b], Qiwei Yang[a,b,*], Zongbi Bao[a,b,*]

[a]Key Laboratory of Biomass Chemical Engineering of the Ministry of Education,

College of Chemical and Biological Engineering, Zhejiang University,

Hangzhou 310027, China;

[b]Institute of Zhejiang University—Quzhou,

Quzhou 324000, China;

‡These authors contributed equally to this work.

*Corresponding author:

Zongbi Bao (baozb@zju.edu.cn); Qiwei Yang (yangqw@zju.edu.cn)

Table of Contents

298K.

Table S1 Lennard Jones parameters of C_3H_6 and C_3H_8.

Table S2 Crystal data and structural refinement.

Table S3 The fitted parameters of the Virial equation for $M(BTFM)(DABCO)_{0.5}$ (M = Zn, Cu).

Table S4 Summary of the adsorption uptake capacity for C_2H_6 and C_2H_4, uptake ratio for C_2H_6/C_2H_4 at 100 kPa and 298 K, and IAST selectivity at 1kPa and 298K on different C_2H_6-selective MOFs.

Table S5 Summary of the adsorption uptake capacity for C_3H_8 and C_3H_6, uptake ratio for C_3H_8/C_3H_6 at 100 kPa and 298 K, and IAST selectivity at 1kPa and 298K on different C_3H_8-selective MOFs.

Table S6 The calculated energies of framework and gas molecules, as well as the binding energies for $Zn(BTFM)(DABCO)_{0.5}$.

Table S7 Equation parameters for the single-site Langmuir-Freundlich isotherms model for C_2H_4 and C_2H_6 adsorption on $M(BTFM)(DABCO)_{0.5}$ (M = Zn, Cu).

Table S8 Equation parameters for the dual-site Langmuir-Freundlich isotherms model for C_3H_6 and C_3H_8 adsorption on $M(BTFM)(DABCO)_{0.5}$ (M = Zn, Cu).

Calculation details

1. Single-component adsorption isotherms

Based on the adsorption isotherms of adsorbates tended to be linear, the single component isotherms of C_2H_4 and C_2H_6 in M(BTFM)(DABCO)$_{0.5}$ (M = Zn, Cu) were fitted with the single-site Langmuir-Freundlich (SSLF) isotherm model[1] (1). While the single component isotherms of C_3H_6 and C_3H_8 in M(BTFM)(DABCO)$_{0.5}$ (M = Zn, Cu) were steep, dual-site Langmuir-Freundlich (DSLF) isotherms model[1] (2) was used to fit these isotherms.

$$q = \frac{bp^c}{1+bp^c} q_{sat} \tag{1}$$

Here, q (mmol/g) is the gas uptake amount in adsorbent, b (kPa^{-1}) represents the affinity coefficient of adsorptive site, c represents the deviations from an ideal homogeneous surface, p (kPa) is the pressure of the bulk gas at equilibrium with the adsorbed phase and q_{sat} (mmol/g) is gas saturation uptake amount. These fitting parameters were provided in the Table S7 with $R^2 > 0.999$.

$$q = \frac{b_A p^{c_A}}{1+b_A p^{c_A}} q_{A\,sat} + \frac{b_B p^{c_B}}{1+b_B p^{c_B}} q_{B\,sat} \tag{2}$$

Here, q (mmol/g) is the gas uptake amount in adsorbent, b_A and b_B (kPa^{-1}) represent the affinity coefficient of adsorptive site A and B, c_A and c_B represent the deviations from an ideal homogeneous surface for adsorptive site A and B, p (kPa) is the pressure of the bulk gas at equilibrium with the adsorbed phase, $q_{A\,sat}$ and $q_{A\,sat}$ (mmol/g) are gas saturation uptake amount at adsorptive site A and B. These fitting parameters were provided in the Table S8 with $R^2 > 0.999$.

2. Separation selectivity of C_2H_6/C_2H_4 mixture and C_3H_8/C_3H_6 mixture

The separation selectivities of C_2H_6/C_2H_4 mixture and C_3H_8/C_3H_6 mixture were calculated with the equation originated from the ideal adsorbed solution theory (IAST).[2]

$$S_{i,j} = \frac{q_i/q_j}{p_i/p_j} \tag{3}$$

Where, $S_{i,j}$ is the selectivity, q_i and q_j are the uptake amount of adsorbates onto the adsorbent in equilibrium with the bulk gas. And p_i, p_j are partial pressure of adsorbates.

3. The isosteric heat of adsorption (Q_{st})

The isosteric heat of adsorption (Q_{st}) for C_2H_4, C_2H_6, C_3H_6 and C_3H_8 of M(BTFM)(DABCO)$_{0.5}$ (M = Zn, Cu) were calculated by means of the adsorption isotherms measured at 273 and 298 K with the Virial-type equation.[3]

$$\ln p = \ln n + \frac{1}{T}\sum_{i=0}^{x} a_i n^i + \sum_{i=0}^{y} b_i n^i \tag{4}$$

$$Q_{st} = -R\sum_{i=0}^{x} a_i n^i \tag{5}$$

Where, p (mmHg) is the pressure, n (mg/g) is the gas uptake amount, T (K) is the temperature, a_i and b_i are the Virial coefficients, x and y are the numbers of coefficients utilized for describing the isotherms, R represents the universal gas constant, and Q_{st} (kJ/mol) is the isosteric heat of adsorption which is independent of the coverage of the adsorbate. The corresponding fitted parameters of the Virial equation for M(BTFM)(DABCO)$_{0.5}$ (M = Zn, Cu) were exhibited in the Table S3.
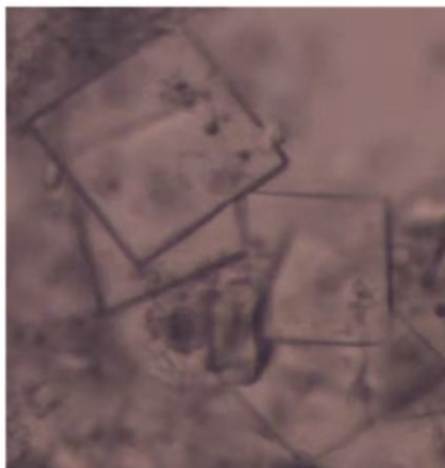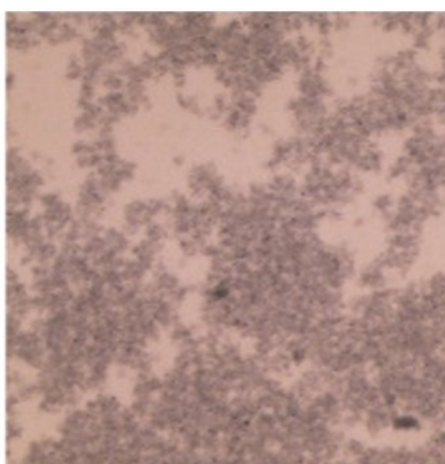
Fig. S1 Optical micrograph of (a) $Zn(BTFM)(DABCO)_{0.5}$ and (b) $Cu(BTFM)(DABCO)_{0.5}$.
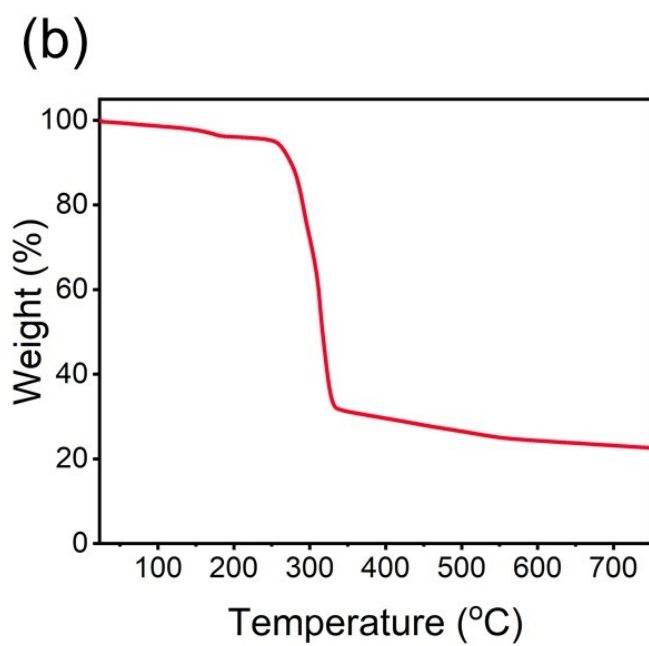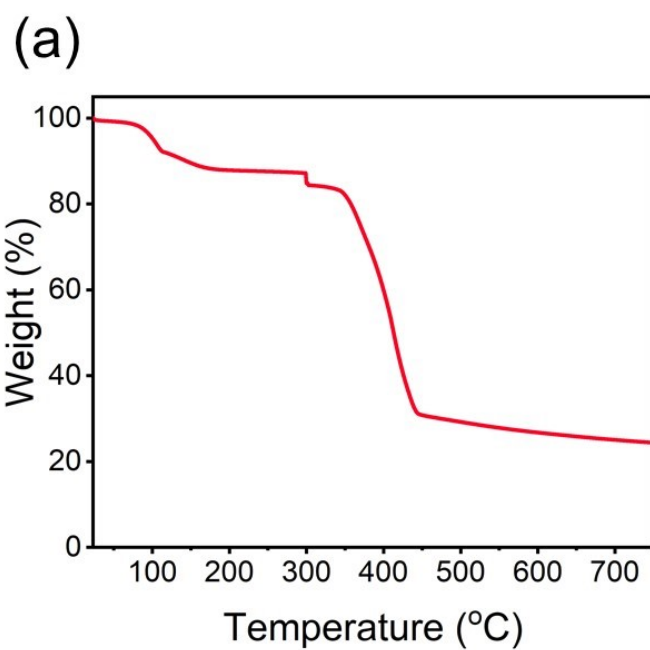
Fig. S2 Thermogravimetric analysis curves of (a) $Zn(BTFM)(DABCO)_{0.5}$ and (b) $Cu(BTFM)(DABCO)_{0.5}$.
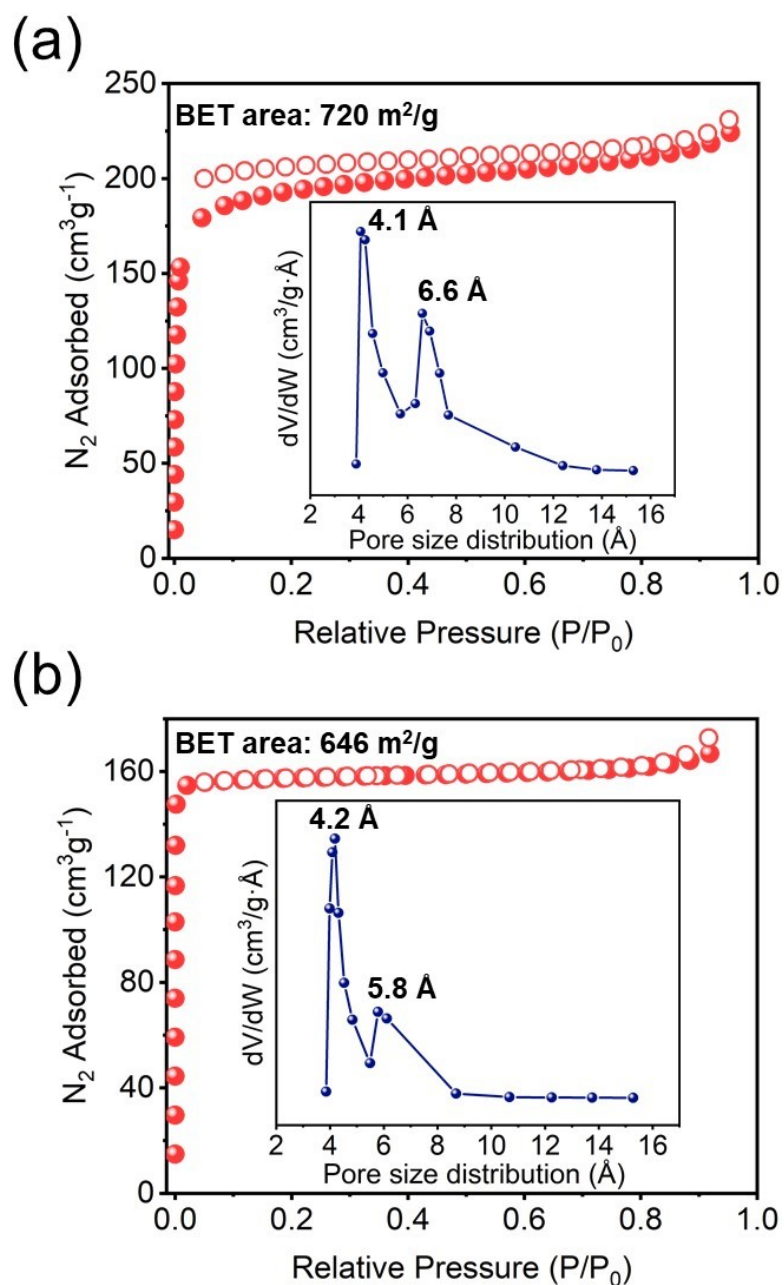
Fig. S3 N_2 adsorption-desorption isotherms at 77 K of (a) Zn(BTFM)(DABCO)$_{0.5}$ and (b) Cu(BTFM)(DABCO)$_{0.5}$. Empty symbols represent N_2 desorption value and inset shows the pore size distribution.
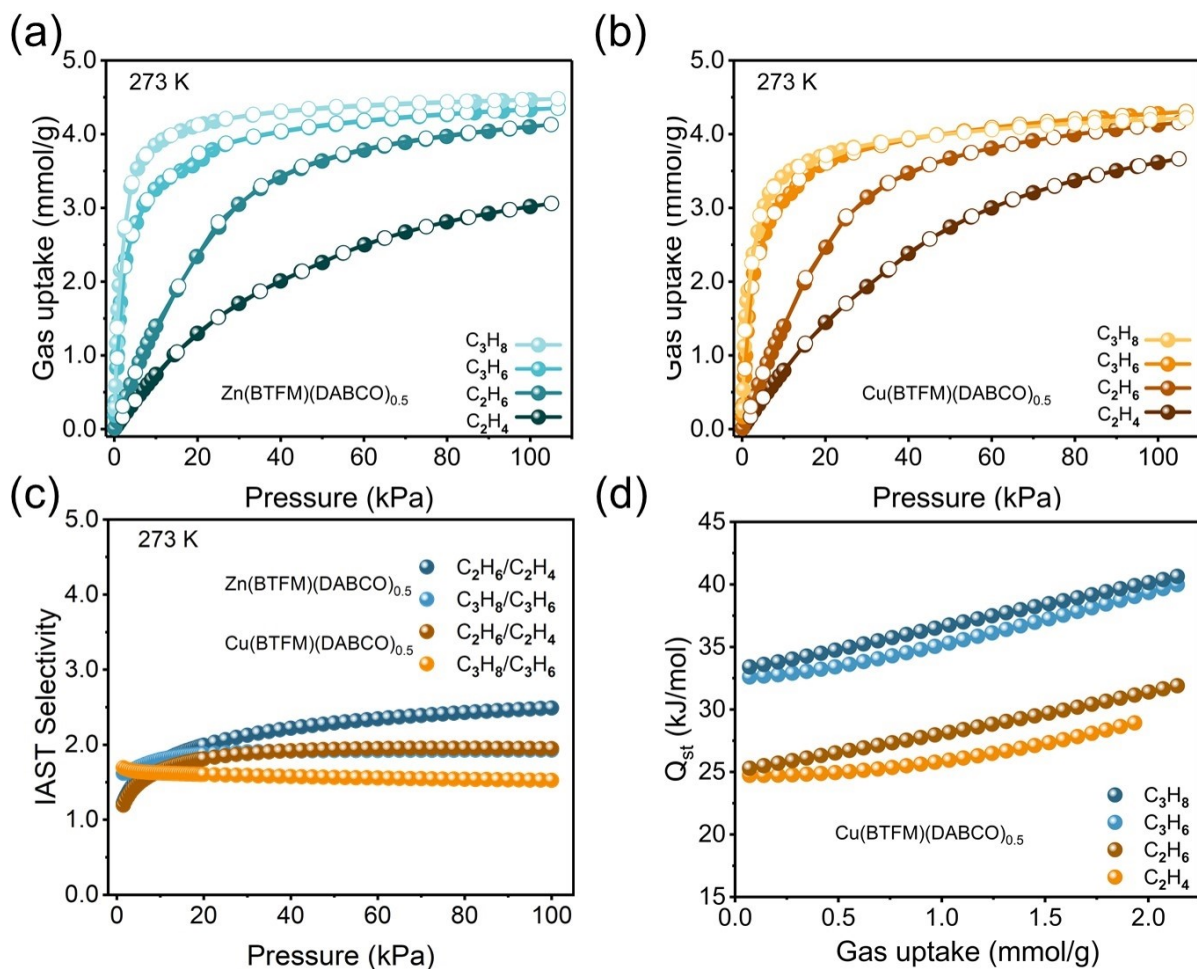
Fig. S4 The C_2H_4, C_2H_6, C_3H_6 and C_3H_8 adsorption isotherms of (a) $Zn(BTFM)(DABCO)_{0.5}$ and (b) $Cu(BTFM)(DABCO)_{0.5}$ at 273 K. (c) The IAST selectivity of C_2H_6/C_2H_4 (50/50, *v/v*) and C_3H_8/C_3H_6 (50/50, *v/v*) at 273 and 298 K for $Zn(BTFM)(DABCO)_{0.5}$ and $Cu(BTFM)(DABCO)_{0.5}$. (d) The adsorption heats of C_2H_4, C_2H_6, C_3H_6 and C_3H_8 adsorbed onto $Cu(BTFM)(DABCO)_{0.5}$.
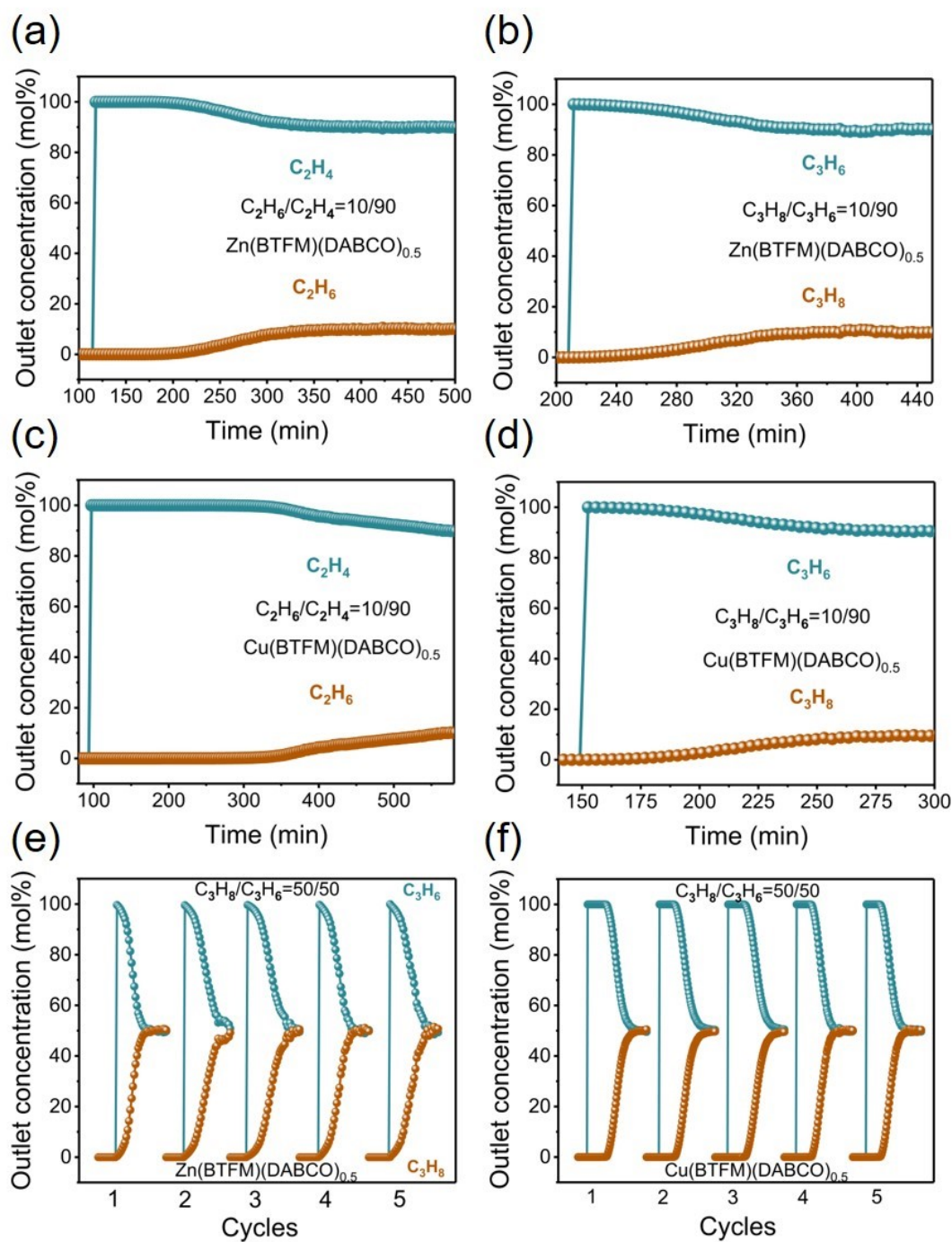
Fig. S5 The experimental breakthrough for (a) C_2H_6/C_2H_4 (10/90, *v/v*) and (b) C_3H_8/C_3H_6 (10/90, *v/v*) in a packed column with activated Zn(BTFM)(DABCO)$_{0.5}$. The experimental breakthrough for (c) C_2H_6/C_2H_4 (10/90, *v/v*) and (d) C_3H_8/C_3H_6 (10/90, *v/v*) in a packed column with activated Cu(BTFM)(DABCO)$_{0.5}$. Five cycles of breakthrough experiments of (e) Zn(BTFM)(DABCO)$_{0.5}$ and (f) Cu(BTFM)(DABCO)$_{0.5}$ for the separation of the C_3H_8/C_3H_6 (50/50, *v/v*) at 298 K and 100 kPa.
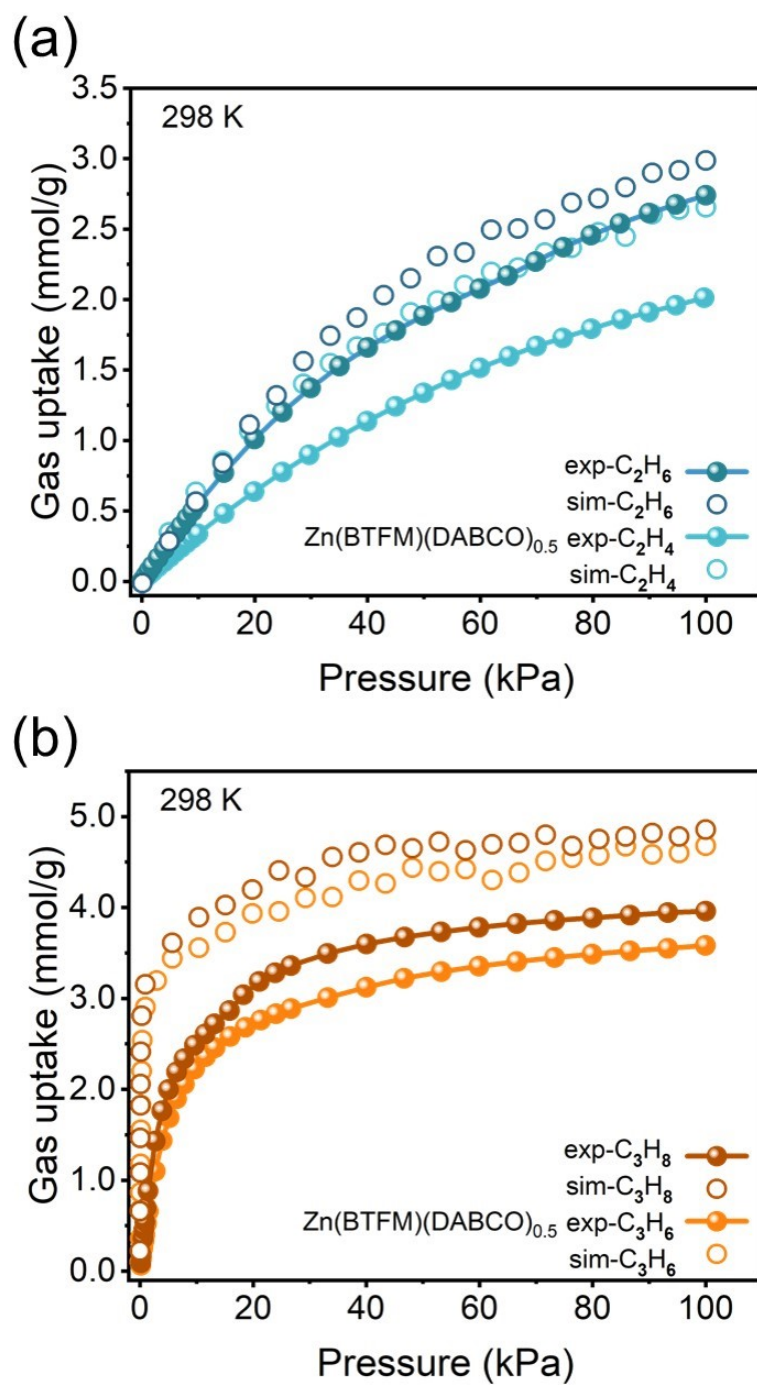
Fig. S6 The experimental and simulated adsorption isotherms of (a) C_2H_4 and C_2H_6 as well as (b) C_3H_6 and C_3H_8 on Zn(BTFM)(DABCO)$_{0.5}$ at 298 K.
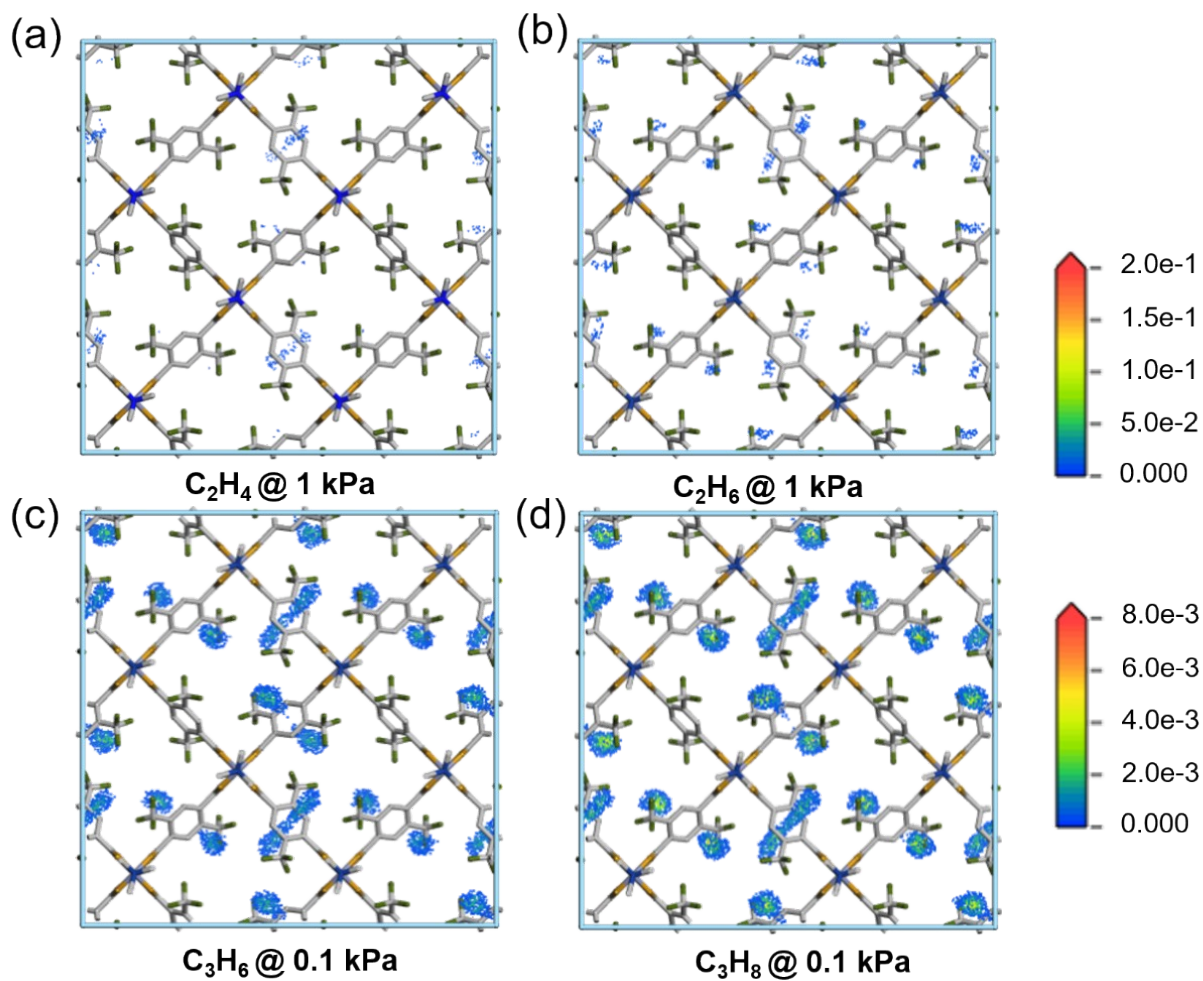
Fig. S7 At 298 K, the density distribution of (a) C_2H_4@1 kPa (b) C_2H_6@1 kPa (c) C_3H_6@0.1 kPa (d) C_3H_8@0.1 kPa on Zn(BTFM)(DABCO)$_{0.5}$. Zn purple, C silvery white, O yellow, F green, respectively. H is omitted for clarity.
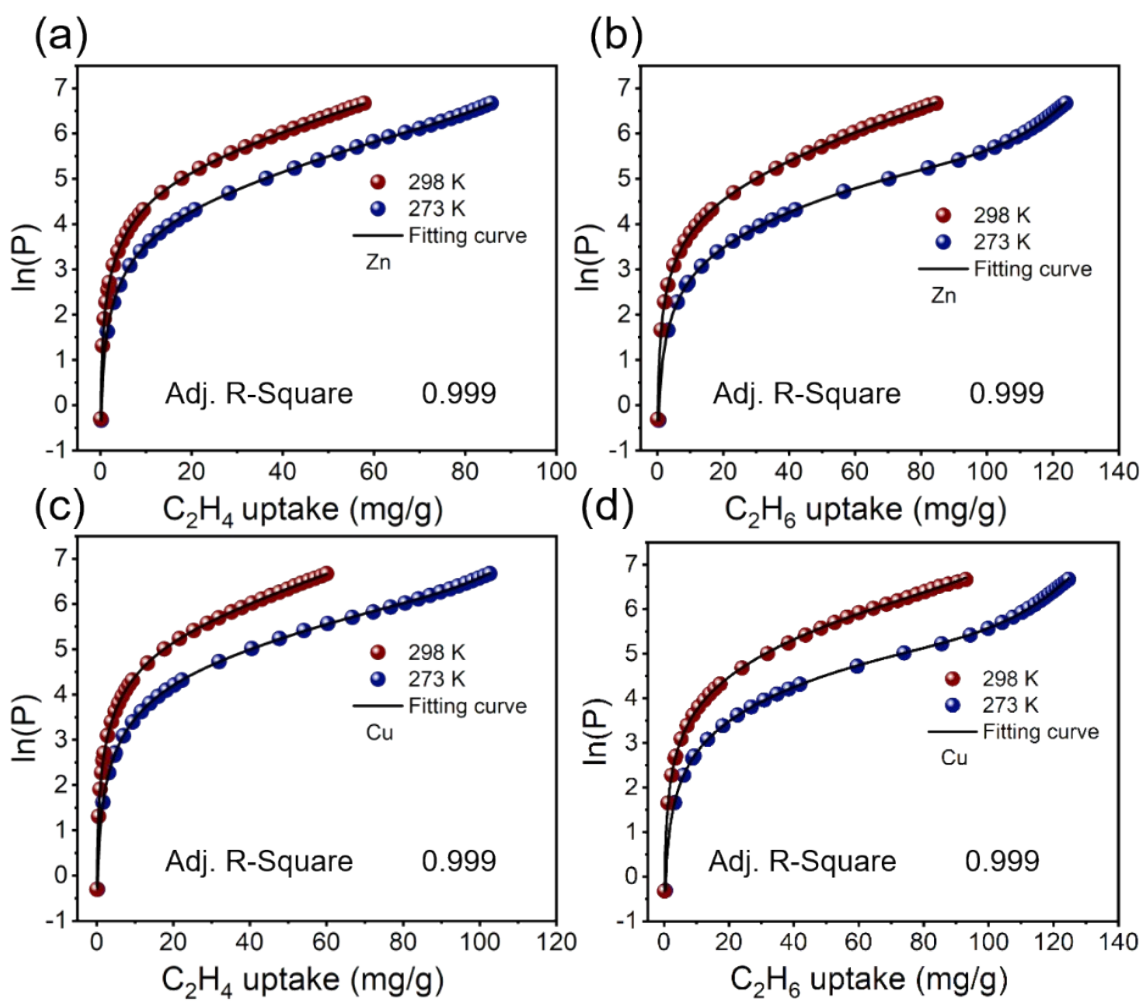
Fig. S8 Virial equation fitting of adsorption isotherms about (a) C_2H_4, (b) C_2H_6 for Zn(BTFM)(DABCO)$_{0.5}$ and (c) C_2H_4, (d) C_2H_6 for Cu(BTFM)(DABCO)$_{0.5}$ at 273 and 298 K.
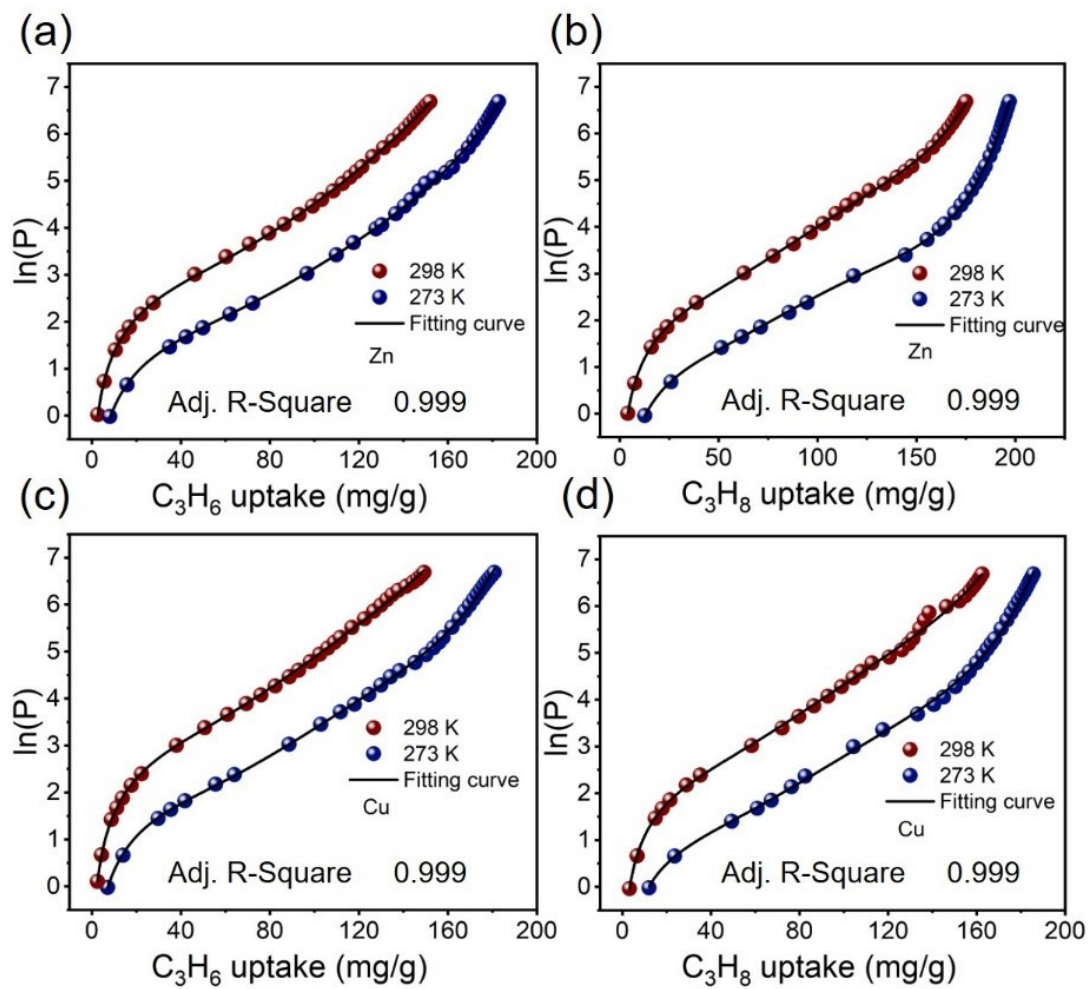
Fig. S9 Virial equation fitting of adsorption isotherms about (a) C_3H_6, (b) C_3H_8 for Zn(BTFM)(DABCO)$_{0.5}$ and (c) C_3H_6, (d) C_3H_8 for Cu(BTFM)(DABCO)$_{0.5}$ at 273 and 298 K.
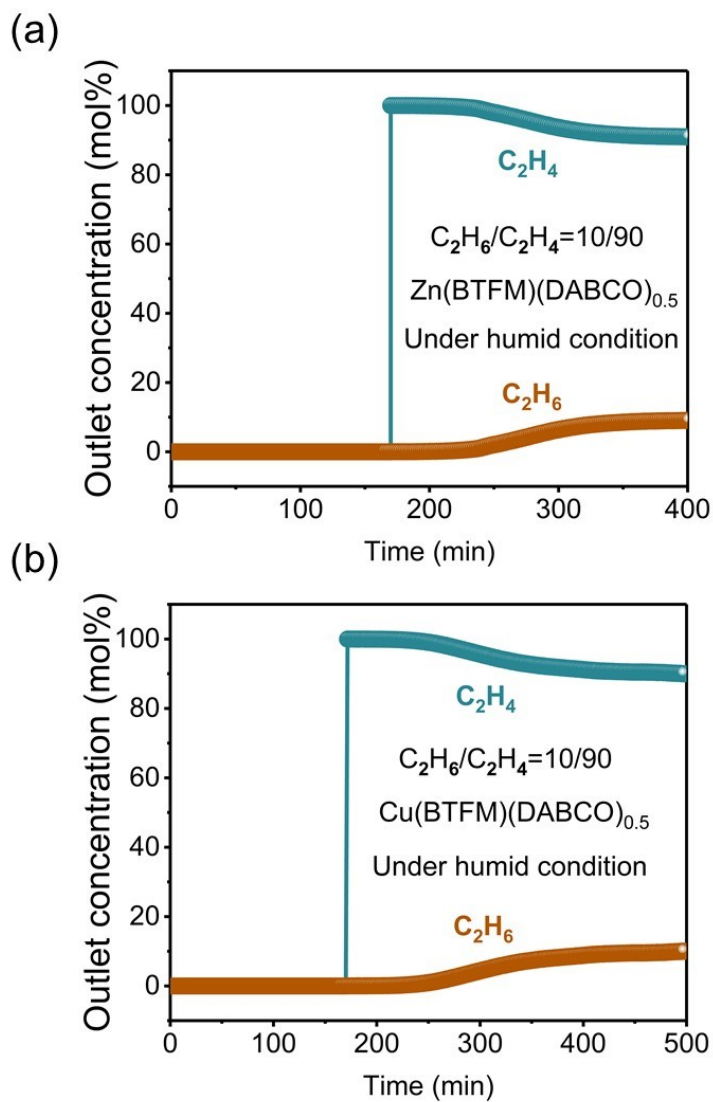
Fig. S10 Breakthrough curves for C_2H_6/C_2H_4 (10/90, *v/v*) on (a) Zn(BTFM)(DABCO)$_{0.5}$ under humid condition and (b) Cu(BTFM)(DABCO)$_{0.5}$ under humid condition at 298 K. The humid condition comes from 10°C pure water bubbled by C_2H_6/C_2H_4 (10/90, *v/v*) gas at a rate of 3 mL/min (49.1% RH, 7530ppm).
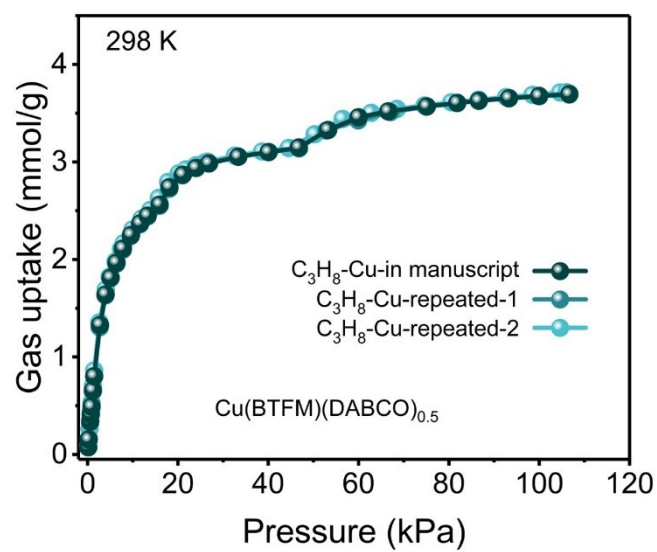
Fig. S11 Repeated experiment data of C_3H_8 adsorption on $Cu(BTFM)(DABCO)_{0.5}$ at 298K.

Table S1 Lennard Jones parameters of C_3H_6 and C_3H_8.

		Atoms	σ (Å)	ε/k_B (K)
Adsorbates	C_3H_6	-CH	3.915	81.89
		-CH$_2$	3.905	89.93
		-CH$_3$	3.915	47.66
	C_3H_8	-CH$_2$	3.905	59.4
		-CH$_3$	3.905	88.1

Table S2 Crystal data and structural refinement.

Crystal	Zn(BTFM)(DABCO)$_{0.5}$	C$_2$H$_4$@Zn(BTFM)(DABCO)$_{0.5}$	C$_2$H$_6$@Zn(BTFM)(DABCO)$_{0.5}$	C$_3$H$_6$@Zn(BTFM)(DABCO)$_{0.5}$	C$_3$H$_8$@Zn(BTFM)(DABCO)$_{0.5}$
Formula	C$_{26}$H$_{16}$F$_{12}$N$_2$O$_8$Zn$_2$	C$_{28}$H$_{20}$F$_{12}$N$_2$O$_8$Zn$_2$	C$_{25}$H$_3$F$_{12}$N$_2$O$_8$Zn$_2$	C$_{14}$H$_{10}$F$_6$NO$_4$Zn	C$_{31.4}$H$_{30.4}$F$_{12}$N$_2$O$_8$Zn$_2$
Molecular weight (g/mol)	843.15	871.24	814.39	435.6	922.52
Space group	P4/n	P4/m	P4/m	P4/mcc	P4/n
a (Å)	15.4464 (11)	10.958 (2)	10.907 (3)	10.9098 (9)	15.4517 (9)
b (Å)	15.4464 (11)	10.958 (2)	10.907 (3)	10.9098 (9)	15.4517 (9)
c (Å)	9.6932 (10)	9.685 (3)	9.688 (3)	19.2797 (17)	9.6409 (5)
α (°)	90	90	90	90	90
β (°)	90	90	90	90	90
γ (°)	90	90	90	90	90
h, k, l	20, 20, 12	12, 12, 11	13, 13, 11	12, 14, 24	18, 18, 11
Cell volume (Å)	2312.7 (4)	1163.0 (6)	1152.5 (7)	2312.7 (4)	2301.8 (3)
Z	2	1	1	4	2
Density (g/cm^3)	1.211	1.244	1.173	1.261	1.331

Table S3 The fitted parameters of the Virial equation for M(BTFM)(DABCO)$_{0.5}$ (M = Zn, Cu).

Parameters	Zn				Cu			
	C_2H_4	C_2H_6	C_3H_6	C_3H_8	C_2H_4	C_2H_6	C_3H_6	C_3H_8
a_0	-2728.30	-3250.90	-3919.59	-4111.38	-2977.70	-3018.39	-3917.14	-3995.51
a_1	-0.010	-9.49	11.62	8.18	1.91	-11.95	-0.87	-7.19
a_2	-0.16	-0.084	-0.30	-0.31	-0.31	0.015	-0.26	-0.13
a_3	0.0035	-0.00016	0.0023	0.0033	0.0037	-0.00041	0.0033	0.0023
a_4	-5.08E-5	-1.28E-5	-1.34E-5	-2.22E-5	-4.16E-5	-2.70E-6	-2.08E-5	-1.69E-5
a_5	2.56E-7	5.42E-8	2.98E-8	5.35E-8	1.73E-7	3.66E-8	4.82E-8	4.37E-8
b_0	11.18	12.32	12.13	12.35	12.06	11.45	12.27	12.17
b_1	0.0063	0.026	-0.028	-0.013	0.0049	0.040	0.020	0.028
b_2	3.14E-4	4.13E-4	5.62E-4	4.52E-4	6.49E-4	1.41E-4	2.61E-4	1.53E-4
Adj. R-Square	0.999	0.999	0.999	0.999	0.999	0.999	0.999	0.999

Table S4 Summary of the uptake capacity for C_2H_6 and C_2H_4, uptake ratio for C_2H_6/C_2H_4 at 100 kPa and 298 K, and IAST selectivity at 1kPa and 298K on C_2H_6-selective MOFs.

MOFs	C_2H_6 (mmol/g)	C_2H_4 (mmol/g)	Uptake ratio (nC_2H_6/nC_2H_4)	IAST selectivity at 1kPa	Ref.
UiO-66-CF$_3$	0.8703	0.4831	1.801	2.6	[4]
ZIF-7	1.888	1.818	1.038	-	[5]
ZIF-8	2.505	1.429	1.753	-	[6]
MAF-49	1.728	1.696	1.020	11.8	[7]
Azole-Th-1	4.462	3.599	1.240	0.78	[8]
Fe$_2$O$_2$(dobdc)	3.296	2.535	1.300	3.76	[9]
JNU-2	4.099	3.502	1.171	1.63	[10]
Ni(TMBDC)(dabco)$_{0.5}$	5.411	4.980	1.086	1.59	[11]
Cu(Qc)$_2$	2.681	1.133	2.365	3.73	[12]
MUF-15	4.374	3.758	1.164	1.96	[13]
IRMOF-8	4.128	3.046	1.355	2.79	[14]
CPM-233	7.395	6.465	1.144	1.21	[15]
ScBPDC	3.417	2.407	1.419	1.03	[16]
MOF-841	4.656	3.442	1.353	1.36	[17]
ZJU-120a*	4.922	3.969	1.240	2.96	[18]
Zn(BTFM)(DABCO)$_{0.5}$	2.740	2.013	1.361	4.53	**This work**
Cu(BTFM)(DABCO)$_{0.5}$	3.017	2.095	1.440	1.82	**This work**

* represents the testing temperature is 296 K.

Table S5. Summary of the uptake capacity for C_3H_8 and C_3H_6, uptake ratio for C_3H_8/C_3H_6 at 100 kPa and 298 K, and IAST selectivity at 1kPa and 298K on C3H8-selective MOFs.

MOFs	C_3H_8 (mmol/g)	C_3H_6 (mmol/g)	Uptake ratio (nC_3H_8/nC_3H_6)	IAST selectivity at 1kPa	Ref.
WOFOUR-1-Ni	1.0	1.2	0.83	2.75	[19]
BUT-10	6.2	6.5	0.95	1.35	[20]
Zr-BPDC	8.4	8.8	0.95	1.48	[21]
Zr-BPYDC	7.2	6.8	1.06	2.79	[21]
CPM-734c	8.7	9.0	0.97	1.08	[22]
MOF-801	3.2	3.5	0.91	1.79	[23]
Ni(ADC)(TED)	2.3	2.1	1.10	3.5	[24]
NUM-7	3.0	3.1	0.97	2.51	[25]
ZIF-8*	4.5	4.6	0.98	-	[26]
Zn(BTFM)(DABCO)$_{0.5}$	4.0	3.6	1.11	1.37	**This work**
Cu(BTFM)(DABCO)$_{0.5}$	3.7	3.6	1.03	1.46	**This work**

* represents the testing temperature is 293 K.

Table S6 The calculated energies of framework and gas molecules, as well as the binding energies for Zn(BTFM)(DABCO)$_{0.5}$.

	Binding energy
E(MOF) (eV)	-40195.57
E(C$_2$H$_4$) (eV)	-380.21
E(C$_2$H$_6$) (eV)	-413.69
E(C$_3$H$_6$) (eV)	-570.96
E(C$_3$H$_8$) (eV)	-604.36
E(MOF+C$_2$H$_4$) (eV)	-40576.12
E(MOF+C$_2$H$_6$) (eV)	-40609.68
E(MOF+C$_3$H$_6$) (eV)	-40767.02
E(MOF+C$_3$H$_8$) (eV)	-40800.47
ΔE(C$_2$H$_4$) (kJ/mol)	-32.44
ΔE(C$_2$H$_6$) (kJ/mol)	-40.76
ΔE(C$_3$H$_6$) (kJ/mol)	-46.98
ΔE(C$_3$H$_8$) (kJ/mol)	-51.98

Table S7 Equation parameters for the single-site Langmuir-Freundlich isotherms model for C_2H_4 and C_2H_6 adsorption on $M(BTFM)(DABCO)_{0.5}$ (M = Zn, Cu).

Framework	Adsorbates	q (mmol/g)	b (kPa^{-1})	c	R^2
Zn	C_2H_4 (298 K)	2.40	0.0045	1.46782	0.999
	C_2H_4 (273 K)	4.39	0.0184	1.04167	0.999
	C_2H_6 (298 K)	4.96	0.0128	0.99075	0.999
	C_2H_6 (273 K)	4.61	0.0246	1.27222	0.999
Cu	C_2H_4 (298 K)	4.82	0.0078	1.00000	0.999
	C_2H_4 (273 K)	5.19	0.0141	1.11268	0.999
	C_2H_6 (298 K)	5.83	0.0114	0.98452	0.999
	C_2H_6 (273 K)	4.52	0.0221	1.34257	0.999

Table S8 Equation parameters for the dual-site Langmuir-Freundlich isotherms model for C_3H_6 and C_3H_8 adsorption on $M(BTFM)(DABCO)_{0.5}$ (M = Zn, Cu).

	Zn				Cu			
	273 K		298 K		273 K		298 K	
	C_3H_6	C_3H_8	C_3H_6	C_3H_8	C_3H_6	C_3H_8	C_3H_6	C_3H_8
q_1 (mmol/g)	3.06	4.37	3.43	1.36	3.41	0.99	3.01	1.64
q_2 (mmol/g)	1.47	0.25	4.00	2.98	1.21	3.33	1.44	2.85
b_1 (kPa^{-1})	0.73	0.67	0.18	0.041	0.21	3.70	0.15	0.33
b_2 (kPa^{-1})	0.02	0.00062	0.00095	0.26	0.96	0.34	0.00040	0.064
c_1	1.23	1.05	1.00	1.00	0.81	1.7	1.15	1.43
c_2	1.25	1.70	1.00	1.00	1.70	0.88	1.7	0.8
R^2	0.999	0.999	0.999	0.999	0.999	0.999	0.999	0.999

References

1   A. L. Myers and J. M. Prusnitz, *AIChE J.*, 1965, **11**, 121-127.

2   K. S. Walton and D. S. Sholl, *AIChE J.*, 2015, **61**, 2757-2762.

3   J. Jagiello, T. J. Bandosz, K. Putyera and J. A, *J. Chem. Eng. Data*, 1995, **40**, 1288-1292.

4   J. Pires, J. Fernandes, K. Dedecker, J. R. B. Gomes, G. Pérez-Sánchez, F. Nouar, C. Serre and M. L. Pinto, *ACS Appl. Mater. Interfaces*, 2019, **11**, 27410-27421.

5   C. Gücüyener, J. van den Bergh, J. Gascon and F. Kapteijn,   *J. Am. Chem. Soc.*, 2010, **132**, 17704-17706.

6   U. Böhme, B. Barth, C. Paula, A. Kuhnt, W. Schwieger, A. Mundstock, J. Caro and M. Hartmann, *Langmuir*, 2013, **29**, 8592-8600.

7   P.-Q. Liao, W.-X. Zhang, J.-P. Zhang and X.-M. Chen, *Nat. Commun.*, 2015, **6**, 8697-8705.

8   Z. Xu, X. Xiong, J. Xiong, R. Krishna, L. Li, Y. Fan, F. Luo and B. Chen, *Nat. Commun.*, 2020, **11**, 3163-3171.

9   L. Li, R.-B. Lin, R. Krishna, H. Li, S. Xiang, H. Wu, J. Li, W. Zhou and B. Chen, Science, 2018, **362**, 443-446.

10   H. Zeng, X.-J. Xie, M. Xie, Y.-L. Huang, D. Luo, T. Wang, Y. Zhao, W. Lu and D. Li, *J. Am. Chem. Soc.*, 2019, **141**, 20390-20396.

11   X. Wang, Z. Niu, A. M. Al-Enizi, A. Nafady, Y. Wu, B. Aguila, G. Verma, L. Wojtas, Y.-S. Chen, Z. Li and S. Ma, *J. Mater. Chem. A*, 2019, **7**, 13585-13590.

12   R. -B. Lin, H. Wu, L. Li, X. -L. Tang, Z. Li, J. Gao, H. Cui, W. Zhou and B. Chen, *J. Am. Chem. Soc.*, 2018, **140**, 12940-12946.

13   O. T. Qazvini, R. Babarao, Z. -L. Shi, Y. -B. Zhang and S. G. Telfer, *J. Am. Chem. Soc.*, 2019, **141**, 5014-5020.

14   J. Pires, M. L. Pinto and V. K. Saini, *ACS Appl. Mater. Interfaces*, 2014, **6**, 12093-12099.

15   H. Yang, Y. Wang, R. Krishna, X. Jia, Y. Wang, A. N. Hong, C. Dang, H. E. Castillo, X. Bu and P. Feng, *J. Am. Chem. Soc.*, 2020, **142**, 2222-2227.

16   S. Jiang, L. Li, L Guo, C. Song, Q. Yang, Z. Zhang, Y. Yang, Q. Ren and Z. Bao, *Sci. China: Chem.*, 2021, **64**, 666-672.

17   S. Jiang, L. Guo, L. Chen, C. Song, B. Liu, Q. Yang, Z. Zhang, Y. Yang, Q. Ren and Z. Bao, *Chem. Eng. J.*, 2022, **442**, 136152.

18   J. Pei, J. Wang, K. Shao, Y. Yang, Y. Cui, H. Wu, W. Zhou, B. Li and G. Qian, *J. Mater. Chem. A*, 2020, **8**, 3613-3620.

19   L. Yang, X. Cui, Q. Ding, Q. Wang, A. Jin, L. Ge and H. Xing, *ACS Appl. Mater. Interfaces*, 2020, **12**, 2525-2530.

20   C. He, Y. Wang, Y. Chen, X. Wang, J. Yang, L. Li and J. Li, *Chem. Eng. J.*, 2021, **403**, 126428.

21   S. Wang, Y. Zhang, Y. Tang, Y. Wen, Z. Lv, S. Liu, X. Li and X. Zhou, *Chem. Eng. Sci.*, 2020, **219**, 115604.

22   A. Hong, H. Yang, T. Li, Y. Wang, Y. Wang, X. Jia , A. Zhou, E. Kusumoputro, J. Li, X. Bu and P. Feng, *ACS Appl. Mater. Interfaces*, 2021, **13**, 52160-52166.

23   P. Iacomi, F. Formalik, J. Marreiros, J. Shang, J. Rogacka, A. Mohmeyer, P. Behrens, R. Ameloot, B. Kuchta and P. L. Llewellyn, *Chem. Mater.*, 2019, **31**, 8413-8423.

24   M. Chang, J. Ren, Y. Wei, J. Wang, Q. Yang, D. Liu and J. F. Chen, *Sep. Purif. Technol.*,

2021, **279**, 119656.

25   S. Q. Yang, F. Z. Sun, R. Krishna, Q. Zhang, L. Zhou, Y. H. Zhang and T. L. Hu, *ACS Appl. Mater. Interfaces*, 2021, **13**, 35990-35996.

26   E. Andres-Garcia, J. López-Cabrelles, L. Oar-Arteta, B. Roldan-Martinez, M. Cano-Padilla, J. Gascon and G. M. Espallargas, *Chem. Eng. J.*, 2019, **371**, 848-856.